AN ACTIVE SURFACE APPROACH FOR SEGMENTATION OF BONE FRAGMENTS IN TRAUMA SURGERY PLANNING

Werner Backfrieder[(a)], Berthold Kerschbaumer[(b)], Gerald Zwettler[(c)]

[(a)]Department of Biomedical Software Engineering
[(b)]Department of Information Engineering and Management
[(c)]Biomedical Research Group
University of Applied Sciences Upper Austria, Hagenberg, Austria

[(a)]Werner.Backfrieder@fh-hagenberg.at, [(b)]Berthold.Kerschbaumer@fh-hagenberg.at,
[(c)]Gerald.Zwettler@fh-hagenberg.at

ABSTRACT
Recent developments of 3D computer technology, as computer graphics, haptic interaction, and 3D rapid prototyping, show promising potential for accurate, patient specific surgical planning. Traumatic surgery may potentially benefit from novel 3D technologies, both in the context of diagnosis and surgical planning. An inevitable prerequisite is accurate morphological segmentation, especially in trauma surgery, where all bone fragments, after a traumatic impact are mostly not clearly distinguishable using common segmentation techniques. A novel method is presented for the separation of these fragment clusters; the concept of adaptive surfaces. A flexible grid of control points is subject to motion, controlled by internal and external attracting forces to assess the outer surface of the bone, applicable for both joints and fractures. Internal forces control the stiffness of the surface and external forces act between the lattice and the landmarks on the bone surface, represented by principal gradient magnitudes. The algorithm yields proper classification of fracture parts and was successfully tested with geometrical phantom data and CT patient data from a heel bone fracture.

Keywords: segmentation, active contours, surgical planning

1. INTRODUCTION
The reconstruction of traumatic fractures is amongst the most challenging tasks in surgery. The number of bone fragments, the disorder caused by the impact, where the parts may be substantially displaced, rotated and even stuffed into each other, need certain experience from the surgeon, as well as a high degree of spatial sense combined with a survey over the surgical situs.
Modern medical imaging devices, e.g. multi-slice CT, provide high resolution 3D image data, allowing accurate diagnosis and staging of the severity of injury. Though there exists a broad spectrum of 3D visualization methods, the systems allowing for manipulation and rearrangement of bone fractures are limited.
The complexity of bone traumata, e.g. fractures of the ankle joint, make it sometimes difficult to reconstruct the original state of morphology and function. Besides these constraints surgery is always a kind of stress situation, requiring distinct decisions in a very narrow temporal slot. Tools for careful identification, repositioning and fixation of bone fragments prior to surgery are desirable and will fit into surgical planning systems (Gorres et al. 2016).
In this work an adaptive surface model is developed to enable the separation of bone fragments after rough pre segmentation by robust methods as thresholding and region growing. The concept of the developed method is in the category of algorithms as evolving or self-adaptive contours, implementing various physical concepts: the propagation of wave fronts (Osher and Sethian 1988), snakes, active contours, and level sets (Bookstein 1996, Wang et al. 1996, Zhu and Yan 1997). The novel segmentation technique is the base for a planning system, comprising general methods for morphological modelling using robust algorithms with little user interaction. The object models are supplied to a manipulation tool, allowing for easy replacement of bone fragments and planning the position of bone plates, screws, and nails.

2. METHODS
The method is applied to a show case of standard CT data taken from a heel bone fracture. Data is acquired on a multi-slice CT, the volume consists of slices with 512x512 pixels, pixel-size 0.72mm x 0.72mm and 0.5mm slice thickness. The number of slices ranges with these type of studies from 300 to 500, thus defines the depth of the volume of interest. Voxel data is represented in Hounsfield units (HU) with 16 bit/voxel.

2.1. Data preprocessing
Image data are reformatted to isotropic voxel-size, i.e. the slice thickness of 0.5mm. Scaling data up in-plane sampling distance is reduced from 0.72mm to 0.5mm, increasing the amount of data roughly by 40%. Cubic spline interpolation is used to calculate the isotropically resampled image data. For display voxel intensities are

rescaled to provide optimal contrast in the bone-window. Bone density shows a wide range of variation, ranging from hard cortical bone (HU=2000) to weakly absorbing spongy bone (HU=300).
A strong prerequisite for generation of accurate models is proper segmentation of all relevant parts. This is challenging, since the wide dynamic range of bone tissue in CT images and the irregular pattern of bone ruptures. The distinction of fragments is complicated by strain of parts into each other.
An edge preserving smoothing filter is applied to flatten intensity variations of image data in order to prepare for segmentation. A locally variant Gaussian shaped linear filter is applied to image data. The filter mask is derived from local gradient magnitude inversely weighted by an edge constant (Li et al. 2009).

2.2. Segmentation

The segmentation is a field of intensive research in medical image processing, where several approaches employing sophisticated mathematical and statistical method were developed (Nascimento and Marques 2005, Liang et al. 2006). Various frameworks are developed for segmentation of abdominal organs (Boes et al. 1994, Campadelli et al. 2010, Muralidhar et al. 2010). In this work a processing pipeline for segmentation of bones, i.e. a semi-automatic classification process under user supervision, is developed, under the constraint of minimal user interaction. It is a hierarchical two-steps process. The first step aims into rough segmentation of all bones contained in the volume of interest (VOI), it is important to identify all bones in the VOI since they build the base for further refinement to achieve final proper segmentation. For this initial segmentation thresholding is applied. The proper threshold values, to distinguish bone from surrounding tissue, are estimated using the optimum thresholding algorithm (Vala and Baxi 2013). The method achieves a large set of voxels representing the main bone morphology, but with no classification of single bones, and traumatic fragments.
This classification is implemented as supervised process with user intervention. The mainly grouped pixel-sets are segmented by seeded region growing. The seed-points are defined manually and the subsequent growing algorithm is realized in 3D. The identification of major well manifested bones is achieved, but a big number of smaller bones are tied together. This is sufficient for all bones not affected by the traumatic event, but to allow careful modelling and surgery planning further, detailed segmentation of the focused fragments is needed.

2.3. Active grid

In many cases the methods described above are not sufficient to achieve object classification of a trauma situs to allow accurate surgical planning. The broken and splintered fragments are partially wedged into each other, or not clearly separated in images, thus clusters of fragments are falsely identify as a single object. Further thresholding or methods from mathematical morphology are not appropriate to achieve final results, thus a novel method, relying on physical principles is developed to isolate the parts by building compartments.

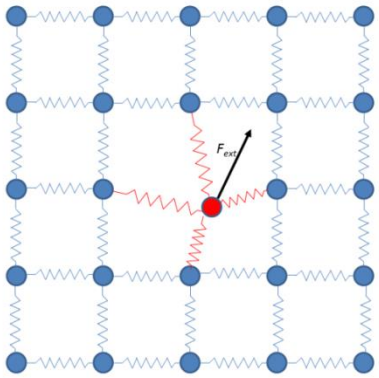

Figure 1: *Sketch of the adaptive grid.*

An adaptive surface is positioned interactively between the fragments. Starting from this initial position the surface is adapted to the shape of the fragments driven by external and internal forces. The external forces attract the surface to the external boundaries of the object; the internal forces control the smoothness of the surface. The active surface is assembled by four-sided patches, cf. Figure 1. Motion and deformation of the surface is controlled by the vertices of the patches. They are arranged on a lattice and joint to each other by springs, controlling the stiffness of the surface. External forces also affect these points, enabling the adaption to morphology. The kind of external force influences convergence and roughness of segmentation, possible choices are:

- spring like linear force,
- $1/r^2$ force like gravity,
- constant force to simulate convection.

Motion is calculated for all mass points during iterative steps. In small time intervals Δt the motion of all grid-points is calculated along the resulting force, corresponding to the equation of motion

$$m\ddot{\vec{x}} = \sum_{i=1}^{N} C_i \left(\|\vec{d_i}\| - l_{0i}\right) \frac{\vec{d_i}}{\|\vec{d_i}\|} + \overrightarrow{F_{ext}} \quad . \qquad (1)$$

The above equation describes the motion of a mass point, accordingly the resulting forces. Acceleration a is the second temporal derivate of the position vector $\vec{x}$, the sum describes the forces generated by the springs, N is the number of adjacent mass points, C_i is the spring constant of the respective conjunction, and l_{0i} is the length of the *i-th* spring in resting state. The vector $\vec{d_i}$ is the distance vector to the neighboring mass point. The external force $\overrightarrow{F_{ext}}$ is chosen in this work as gravity like force of the form

$$\overrightarrow{F_{ext}} = \sum_{j} G \frac{M_j m}{\|\vec{r_j}\|^2} \frac{\vec{r_j}}{\|\vec{r_j}\|} \quad . \qquad (2)$$

It sums up the attraction forces of all surface bound mass points M_j of interest, i.e. morphological landmarks, where $\vec{r_j}$ is the distance vector from the actual grid point to these morphological landmarks. The constant G and the fictive masses M_j allow the fine tuning of the algorithm. Since this type of external force reaches infinity when the distance approaches zero, a limit corresponding to a minimal distance r_{min} is defined, to avoid accidental sticking of the surface at some random landmarks, especially when the separation of two parts is desired and the surface has to fit into a small gap.

The morphological landmarks are generated by calculating the magnitude of gradients. To restrict the landmarks to points of the surface, thresholding is performed and the number of landmarks is reduced. The magnitude of the gradient is a guess for the mass of the landmark.

Calculating the evolution of the lattice is a very complex multi object problem, but the observation of small time intervals allow the linearization of the problem and thus decoupling of the multi body system. During a single iteration the trajectory of a grid point along its resulting acceleration vector is calculated. The iteration is completed when all grid points have been considered. This simplification allows easy computation but yields very realistic motion behavior.

For special purposes, e.g. the separation of loosely connected bone particles, selected grid points may be defined as static. This means, they remain at their initial positions; usually the outer borders of the lattice are defined static, building a stationary frame for the evolving surface. But also some arbitrary point of the lattice may be fixed to the bone surface, i.e. some kind of pretension of the surface, to further accelerate the evolution to the final segmentation form.

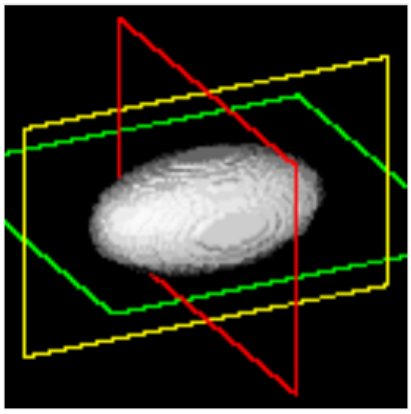

Figure 2: *Volume rendering of the ellipsoid phantom data set. The green, red and yellow frames indicate the axial, coronal and sagittal cutting planes.*

3. RESULTS

The active grid concept is demonstrated with simulated phantom data and a showcase of clinical data, the comminuted fraction of a heel bone.

3.1. Phantom data

Phantom data represent a homogeneous ellipsoid positioned at the center of a 128x128x80 image volume of isotropic voxels. The lengths of half axis are 40, 20, and 20 pixels. A volume rendering of the data set is shown in Figure 2.

Landmark points upon the surface are calculated using an unsharpen enhance filter. To speed up calculation and to easily exclude distant points, further than a certain threshold, a potential map is generated, based on the surface landmarks. In this case the potential field is calibrated to zero at the landmarks and a simple Euclidean distance field is applied. The three major cutting planes through the center of the potential field are displayed in Figure 3.

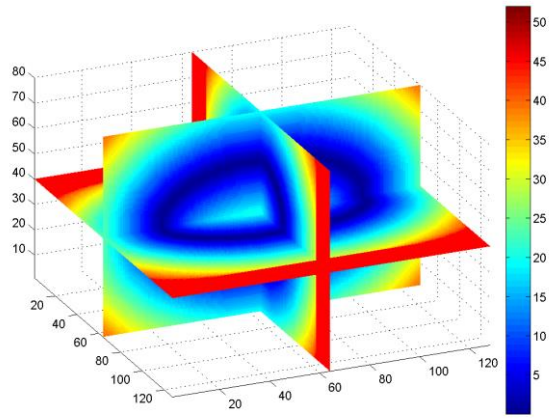

Figure 3: *Potential field of the ellipsoid's surface landmarks. A simple Euclidean distance metrics is implemented. The field values are limited to 45.*

A grid with 11x11 equally spaced control points is positioned in coronal orientation cutting the first quarter of the long axis of the ellipsoid. The four corner points of the grid are defined *static*. In Figure 4.a the grid is depicted, superposed to a transparent axial plane through the center of the ellipsoid. The opacity value of the plane is 0.7. After an evolution of 1000 iterations along the negative gradients of the potential field, the deformed plane yields its final shape. It is positioned exactly on the border landmarks of the ellipsis, cf. Figure 4.b.

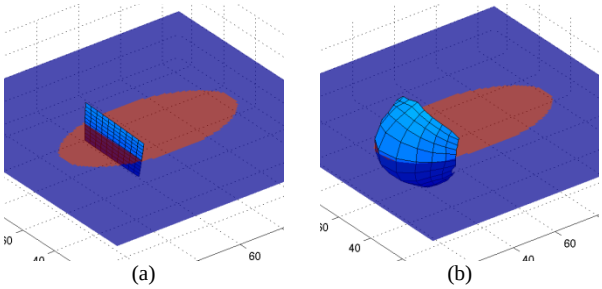

(a) (b)

Figure 4: *Evolution of the grid. A grid with 11x11 control points, fixed at the four corners, evolves 1000 steps along the descending gradient of the potential field. The initial position (a) and the final position (b) are depicted.*

3.2. Patient data

Real patient data, as acquired prior to surgery, are usually contaminated with modality inherent noise. Noise reduction and emphasis of edges in image data facilitate successful segmentation with the evolving surface algorithm. During the first processing step image data is smoothed. The effect of the edge preserving adaptive filter is shown in Figure 5, with different settings of the edge parameter and the mask size. The native image is shown in Figure 5.a, the slice is slightly below the ankle, and thus the metatarsal bones are shown on top, followed by the tarsal bones and finally the fractured calcaneus (heel bone). The images (b) and (c) are calculated with mask size 3x3 and 10% and 40% of maximal gradient magnitude. The results with mask size 5x5 and 10% magnitude scaling are shown on the right in sub-image (d).

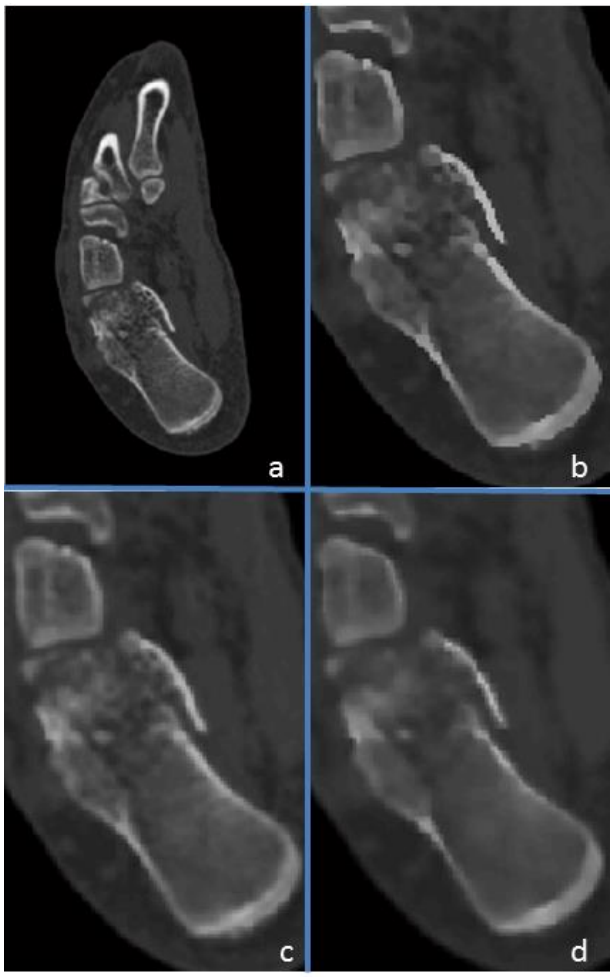

Figure 5: *Edge preserving smoothing with different parameter settings for mask size and edge strength.*

The results of the pre-segmentation step are shown in Figure 6. A simple thresholding followed by a seeded region growing is performed. The method is sufficient for accurate separation of soft tissue and bones, but classification of all bones as separable objects, as required by a planning system, is not achievable.

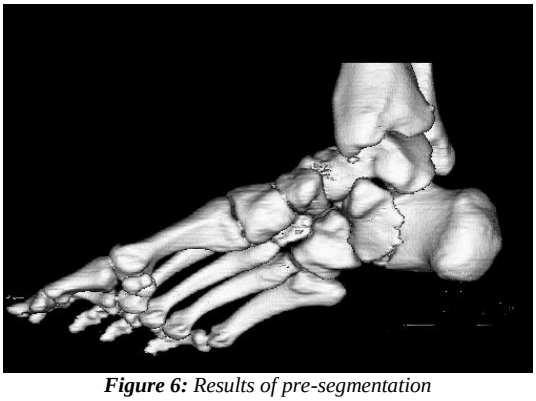

Figure 6: *Results of pre-segmentation*

The potential field yielded from the surface of the pre-segmented volume is shown in Figure 7, three perpendicular representative slices through the image volume are displayed.

The active grid approach, based on the primary segmentation, keeps the chosen thresholds. Increasing thresholds are in most cases along with the erosion of substantial parts of bone morphology, not tolerable with accurate reconstruction of the injured extremity. The feasibility for the active grid segmentation approach is demonstrated with tarsal bones and the upper ankle joint. The position of the initial 15x15 grid is shown in Figure 8.a on top of two transparent perpendicular slices, with opacity value 0.7. It is manually localized by defining the four vertices. In its initial position it traverses the ankle bone (talus), thus only the uncovered edges are clearly visible. The final surface is shown after 1000 iterations with a time increment of 0.2s, cf. Figure 8.b. It fits exactly into the joint gap and

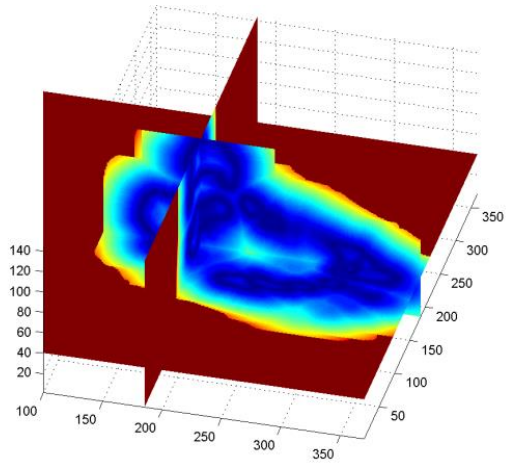

Figure 7: *Potential field of the landmarks at the bone surfaces of the CT examination of the heel bone fracture.*

facilitates easy separation of the talus and the shinbone (tibia). The applicability of the method is also demonstrated with smaller joints in the tarsal area. The position of the manually defined, initial 11x11 lattice is shown in Figure 9.a. The result after 1000 iterations merely fits to the shape of the tarsal bone and defines a distinct border for separation of both parts, cf. Figure 9.b.

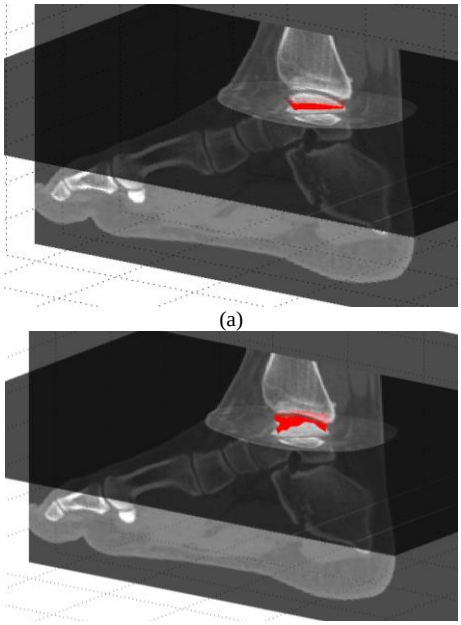

(a)

(b)

Figure 8: *Segmentation of tibia and talus with the active grid approach. The lattice is drawn red at its initial position (a) and after 1000 iterations it fits perfectly into the gap between the bones (b). The grid is drawn over two perpendicular cutting planes, with an alpha value of 0.7.*

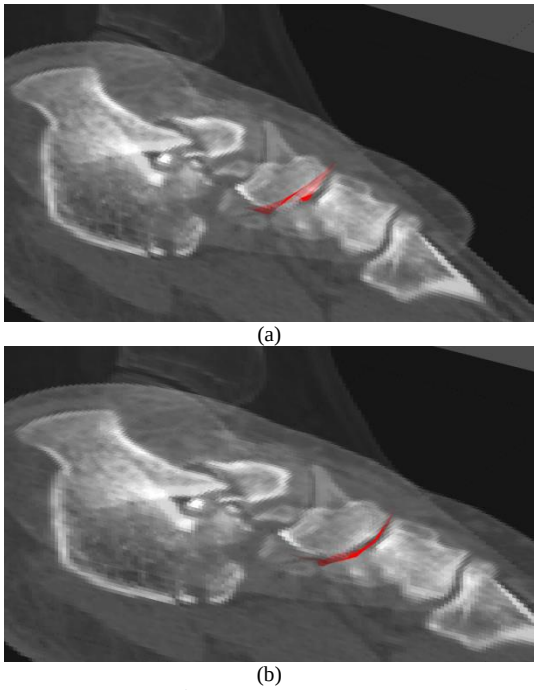

(a)

(b)

Figure 9: *Separation of tarsal bones. A 10x10 lattice (red) at the initial position (a) and after 1000 iterations with time constant 0.2s it perfectly masks the joint surface (b).*

The final result of segmentation achieved with the adaptive surface algorithm is depicted in Figure 10. The mainly linked bone morphology, obtained by pre-segmentation with thresholding and region growing is further separated in detail, employing the adaptive surface method. The colored segments are shown in Figure 10, the heel bone is represented in olive color, the fragments of the heel bone are colored blue and turquoise, the broken and displaces tarsal bone is shown in red. The bone is rotated in such a way that the joint surface is oriented backwards.

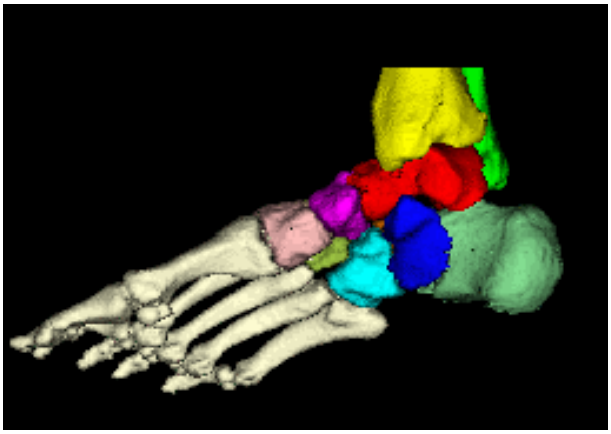

Figure 10: *Final result of adaptive surface segmentation*

4. DISCUSSION

A novel segmentation algorithm employing an active layer for proper separation of pre-segmented bone fragment is presented. The algorithm is integrated into a pipeline of sophisticated image processing steps, facilitating accurate 3D surgical planning. The algorithm is mainly designed to separate agglomerated bones from each other, after a rough pre-segmentation step. It differs from existing approaches like active contours or snakes, since the internal forces operating on grid nodes are solely attracting forces. They provide no stiffness to the evolving surface, thus a close approximation to the given surface is possible. The adaption to the surface is mainly achieved by the external forces. This composition has certain potential to remove random outliers from the resulting segmented parts. Furthermore this design of internal forces is suitable to fit into small joint spaces, the approximation is only controlled by the adjacent joint surfaces and the internal forces just act as shear forces to optimize the energy within the grid.

In further work the influence of weighting the surface landmarks with scene dependent point loads and the choice of other potential functions on the convergence of the method will be investigated.

ACKNOWLEDGMENTS

Authors gratefully thank Dr. Christian Rodemund from the AUVA Emergency Hospital Linz for providing image data and detailed useful discussion.

REFERENCES

Evans W.A., 1994. Approaches to intelligent information retrieval. Information Processing and Management, 7 (2), 147–168.

Osher, S.; Sethian, J. A., 1988. Osher, S.; Sethian, J. A. (1988), "Fronts propagating with curvature-dependent speed: Algorithms based on Hamilton–Jacobi formulations" , J. Comput. Phys. 79: 12–49

Boes, J.L., Bland, P.H., Weymouth, T.E., Quint, L.E., Bookstein, F.L., Meyer, C.R., 1994. Generating a normalized geometric liver model using warping. Invest Radiol. 1994 Mar;29(3):281-6.

Bookstein, F.L., 1996. Biometrics, biomathematics and the morphometric synthesis. Bull Math Biol. 1996 Mar;58(2):313-65.

Campadelli, P., Casiraghi, E., Pratissoli, St., 2010. A segmentation framework for abdominal organs from CT scans. Artif Intell Med. 2010 Sep;50(1):3-11.

Gorres, J., Brehler, M., Franke, J., Vetter, S.Y., Grutzner, P.A, Meinzer, H.-P., Wolf, I., 2016. Articular surface segmentation using active shape models for intraoperative implant assessment. Int J Comput Assist Radiol Surg. 2016 Apr 19.

Li, Q., Wang, B., Fan, S.; 2009. An Improved CANNY Edge Detection Algorithm. In 2009 Second International Workshop on Computer Science and Engineering proceedings : WCSE 2009 : 28–30 October 2009, Qingdao, China, pp. 497–500.

Liang, J., McInerney, T., Terzopoulos, D., 2006. United snakes. Med Image Anal. 2006 Apr;10(2):215-33.

Muralidhar, G.S., Bovik, A.C., Giese, J.D., Sampat, M.P., Whitman, G.J., Haygood, T.M., Markey, M.K., 2010. Snakules: a model-based active contour algorithm for the annotation of spicules on mammography. IEEE Trans Med Imaging. 2010 Oct;29(10):1768-80.

Nascimento, J.C., Marques, J.S., 2005. Adaptive snakes using the EM algorithm. IEEE Trans Image Process. 2006 Mar;15(3):788

Vala, H.J., Baxi, A., 2013. A review on Otsu image segmentation algorithm. International Journal of Advanced Research in Computer Engineering and Technology (IJARCET) 2 (2): 387

Wang, M., Evans, J., Hassebrook, L., Knapp, C., 1996. A multistage, optimal active contour model. IEEE Trans Image Process. 1996;5(11):1586-91.

Zhu, Y., Yan, H., 1997. Computerized tumor boundary detection using a Hopfield neural network. IEEE Trans Med Imaging. 1997 Feb;16(1):55-67

AUTHORS BIOGRAPHY

Werner Backfrieder received his degree in Technical Physics at the Vienna University of Technology in 1992. Until 2002 he was with the Department of Biomedical Engineering and Physics of the Medical University of Vienna, where he focused on Medical Image Processing and time series analysis in Nuclear Medicine. Since 2002 he is with the University of Applied Sciences Upper Austria at the division of Biomedical Informatics. His research focus is on Medical Physics and Medical Image Processing in Nuclear Medicine and Radiology with emphasis to high performance computing. Recent research efforts are laid on virtual reality techniques in the context of surgical planning and navigation.

Berthold Kerschbaumer was born in Steyr, Austria and studied at the Johannes Kepler University in Linz, where he received his degree at the Faculty of Social Sciences, Economics and Business in 1993. Then he was with the Department of Data Processing were he got his PhD in 1997 and reached a tenure position in 1997. From 1999 to 2002 he was head of a leading internet software company and since 2002 he is with the University of Applied Sciences Upper Austria at the division of Software Engineering. His research focus is on eBusiness , Information Management and the history of office automation.

Gerald A. Zwettler was born in Wels, Austria and attended the Upper Austrian University of Applied Sciences, Campus Hagenberg where he studied software engineering for medicine and graduated Dipl.-Ing.(FH) in 2005 and the follow up master studies in software engineering in 2009. In 2010 he has started his PhD studies at the University of Vienna at the Institute of Scientific Computing, where he received his degree in December 2014. Since 2005 he is working as research and teaching assistant at the Upper Austrian University of Applied Sciences at the school of informatics, communications and media at the Campus Hagenberg in the field of medical image analysis and software engineering with focus on computer-based diagnostics support and medical applications.